Investigation of Electrostatic Shieldings in Traction Motors to Mitigate Capacitive Bearing Currents

Silvan Scheuermann
Institute of Electrical Engineering (ETI)
Karlsruhe Institute of Technology (KIT)
Karlsruhe, Germany
silvan.scheuermann@kit.edu

Matthias Brodatzki
Institute of Electrical Engineering (ETI)
Karlsruhe Institute of Technology (KIT)
Karlsruhe, Germany
matthias.brodatzki@kit.edu

Martin Doppelbauer
Institute of Electrical Engineering (ETI)
Karlsruhe Institute of Technology (KIT)
Karlsruhe, Germany
martin.doppelbauer@kit.edu

***Abstract*—Electrostatic shieldings in electrical machines have the capability to mitigate harmful capacitive bearing currents. By employing Finite Element (FE)-simulations, the shieldings' effectiveness, influence on parasitic capacitances, and the associated eddy current losses are investigated. The study includes various shielding designs for both, the stator and end-winding part of a motor. Based on the knowledge gained by the Finite Element Analysis (FEA), motorettes with slot-shieldings and stators with overhang shieldings were built. Finally, the study presents the validation of the slot-shieldings' effectiveness by impedance measurements. The measurements confirm a reduction of the winding-rotor capacitance up to approx. $84\,\%$. A large focus is given to the development of an appropriate design regarding its suitability in series production.**

***Index Terms*—Electric machines, Traction motors, Bearing currents, Parasitic effects, Bearing damage, Finite Element Analysis**

I. Introduction

Drive systems, not only traction motors, are mainly fed by inverter systems with employed pulse width modulation (PWM) technique. The current trends in power electronic systems, in mean of SiC-MOSFET or GaN- technology, are attracted by many benefits. Especially the fast switching frequencies contribute to higher efficiency rates in comparison to Si-IGBTs [1]. With these benefits also parasitic effects of switching transients due to square-wave pulses with steep and high voltage edges can occur. Regarding the motors' bearings, the capacitances between the inner and outer raceways create a voltage divider proportional to the inverter-induced common-mode (CM) voltage at the motors' terminal. The capacitive voltage divider, or Bearing-Voltage-Ratio (BVR) in (1) represents the ratio between the bearing voltage u_B and the CM-voltage u_CM [2].

$$\mathrm{BVR}=\frac{u_\mathrm{B}}{u_\mathrm{CM}}=\frac{C_\mathrm{WR}}{C_\mathrm{B,DE}+C_\mathrm{SR}+C_\mathrm{WR}+C_\mathrm{B,NDE}} \tag{1}$$

Refer to (1), the BVR can be estimated by dividing the winding-to-rotor capacitance C_WR by the sum of the stator-to-rotor capacitance C_SR, the bearings' capacitances of the drive- ($C_\mathrm{B,DE}$) and non-drive-end ($C_\mathrm{B,NDE}$), and the winding-to-rotor capacitance (C_WR) [3].

Breakdowns of the capacitances may lead to electric discharge currents and further lead to a meltdown or vaporization of the bearings' materials or lubrication. Micropittings in the bearings' raceways, corrugated patterns, grey surfaces, and other erosive effects are indicators of electrical stress in bearings [4].

Besides the capacitive bearing currents, the common classification in literature [3] categorizes the harmful bearing currents in inverter-fed motors in Electric Discharge Machining (EDM)-, High-Frequency (HF)-circulating-, and HF-rotor-to-ground-bearing currents. But bearing currents can occur also in line-operated motors. These classical types are circulating bearing currents at low frequency and caused by magnetic asymmetries within the motor [3].

There are already numerous ways to prevent bearing damage and potentially failure of the entire drive system as a consequence of capacitive bearing currents. However, they are often not applicable due to their cost, effectiveness, and feasibility. Roughly, these measures can be divided into bearing insulation, shaft grounding, rotor shielding, or common-mode filters [5]–[8]. Additionally, in the international standard IEC/TS 60034-25:2014 [9], a table summarizes the main mitigation techniques and highlights which type of bearing currents is addressed by one solution [8].

II. Physical principles of the shielding

The primary purpose of electrostatic shielding is to minimize electrostatic coupling between the winding and rotor, isolating the rotor from common-mode voltage. A Faraday's cage by embedding a conductive electrode between the stator and the rotor is seen as a practical solution to put in practice. Ideally, the shielding covers both, the stator and end-winding part of a motor. The shielding of the stator lamination part can either be placed in the slot or in the air gap between the winding and the rotor. The other, in the winding's overhang, prevents the capacitance between the bent end-winding-conductors and the rotor's end shields or rotor shaft. All measures have the goal to prevent the electric field between the winding and the rotor, which corresponds to the reduction of the winding-to-rotor capacitance C_WR [10]. However, with the shielding, a new capacitance C_ShR between the shielding and the rotor is introduced, which forms an electrical circuit with the capacitances of the bearings C_B. Fig. 1 shows the

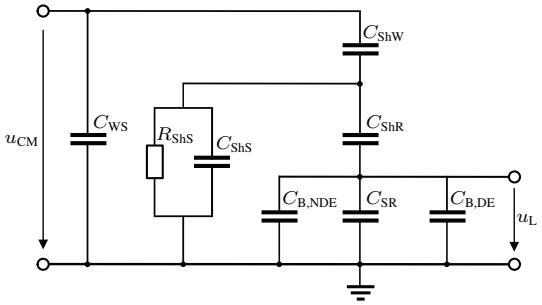

Fig. 1: Equivalent circuit of the parasitic motor structure with shielding measures

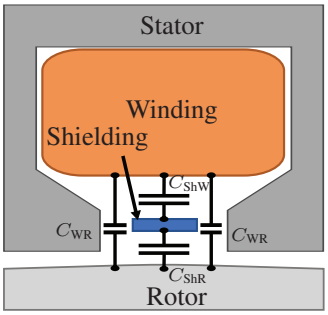

Fig. 2: Schematic representation of the slot-shielding part

equivalent circuit to analyze the new parasitic behavior of the electrical machine.

Moreover, since the shielding is grounded, the connection to the ground is described by the parallel resistance R_{ShS} in the equivalent circuit of Fig. 1. If the grounding connection is ideal, the shaft voltage becomes zero, because the capacitive voltage divider from the shielding to the rotor respectively the stator is short-circuited. If the connection resistance is very high, so that $R_{ShS} \to \infty$, the connection can be seen as an open circuit. In this case, the estimation formula for the BVR becomes (2). It indicates already a reduction in the voltage over the bearings, because the capacitance C_{ShR} is much lower than C_{RE} [11].

$$\mathrm{BVR}_{ShR} = \frac{C_{ShR} \cdot C_{ShW}}{(C_{RE} + C_{ShR}) \cdot \left(C_{ShS} + C_{ShW} + \frac{C_{RE} \cdot C_{ShR}}{C_{RE} + C_{ShR}} \right)} \tag{2}$$

with: $C_{RE} = C_{B,DE} + C_{SR} + C_{B,NDE}$

In summary, from the analytical estimation, the best solution to prevent shaft voltages is a very low, ideal resistive connection from the shield to the ground so that the formerly capacitive voltage divider in (1) is short-circuited [11]. Further, to fulfill its function, the shielding must be made of conductive material and has to be insulated from other components. As e.g. [11], [12] show, the shielding has to be grounded on one end only, since otherwise conductor loops and hence eddy currents, in mean of the working principle in induction motors, are formed.

III. Design and Material Choice of the Shielding

In the following, to evaluate the effectiveness of the shielding, the chosen designs and materials of the shieldings in the stator and overhang part are presented. The study pertains to a series permanent magnet traction motor with hairpin windings and a rated power of approx. 90 kW. The width of the slot opening is 1.4 mm, the stator stack length is 105 mm. To achieve more stable measurement results, and from experience in capacitance measurements, the shielding measures were validated with motorettes with rescaled slot geometry sizes. Thus, the slot opening was extended to 5 mm, the motorettes' stack length remain 105 mm.

A. Slot-shielding

The effect of the slot-shielding part can be analytically determined by Fig. 2, in which all capacitances are assumed as plate capacitances.

The plate capacitance equation in (3) can estimate the remaining capacitance between the winding and the rotor C'_{WR}.

$$C'_{WR} = \varepsilon_0 \varepsilon_r \frac{(b_{Slot} - b_{Sh}) \cdot l}{d_{WR}} \cdot N_{Slot} \tag{3}$$

Thereby, $(b_{Slot} - b_{Sh})$ describes the remaining effective width for the electric field, d_{WR} represents the distance between the winding and the rotor, l denotes the length of the stator lamination stack and N_{Slot} specifies the number of slots of the motor. Hence, (3) depicts the direct influence of the slot-shielding's width b_{Sh} on the capacitance C'_{WR}.

To investigate the slot-shielding measures, one of the built motorettes contains of five slots. The first slot was used as reference, without any shielding measure. In the other slots, slot shieldings with the geometric properties, described in Table I, were embedded. The first slot-shielding design is a copper foil and the second is a copper sheet metal strip. Both of them are enveloped in insulation material to secure the insulation requirement from other components. In the other two slots, either an already enameled flat copper wire or an enameled round copper wire was implemented, as such are commonly used for motor windings.

TABLE I: Geometric properties of the slot-shieldings

Description	***Slot 2***	***Slot 3***	***Slot 4***	***Slot 5***
Type	Foil	Strip	Flat wire	Round wire
Dimensions	t=0.05 mm	4.8x1 mm	2.3x0.85 mm	d=1.6 mm
Material	Copper			
Insulation	Paper	Paper	Enameled	Enameled

In the second motorette, which was built up, a conductive glow protection material is embedded. The choice was made because the shielding in one slot is very close to the winding and the safety requirements according to the DIN EN 60204-1 standard must be fulfilled [13]. The materials for this study have a surface resistance of 1000 Ω/□. Thus, they are less

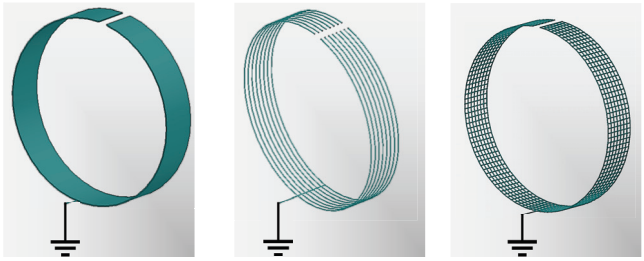

(a) Grounded conductive band (b) Grounded parallel rings (c) Grounded Faraday's cage

Fig. 3: Examples for overhang-shielding variants [12]

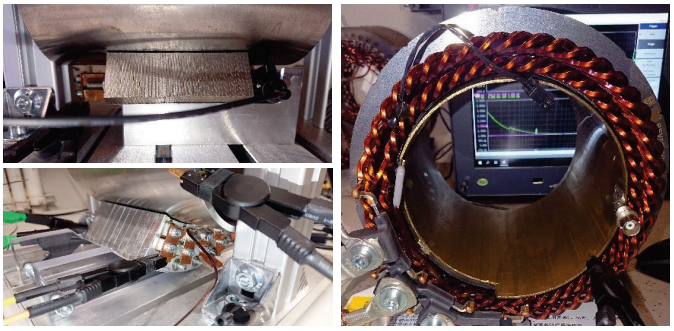

(a) Slot-shielding test setup (b) Overhang-shielding test setup

Fig. 4: Test setup for shieldings' effectiveness validation

conductive than copper, but they fulfill the safety requirements in regard to series development.

B. Overhang-shielding

Since the electric field between the stator windings and the rotor in the overhang part is allowed to form freely, unrestricted by any additional geometrical contractions, a large surface shield is necessary. Examples for the overhang-shielding are shown in Fig. 3 [12]. The variant (a) in Fig. 3 seems to be the most effective solution, but because of the surrounding magnetic field and thus in such kind of conductive closed structures, the induced eddy currents are critical [12]. Design variant (b) represents several grounded loops in parallel. The Faraday's cage principle as in Fig. 3 (c) is used in various applications to shield devices from disturbing electromagnetic fields. If it is placed in between electrical fields, it also mitigates the capacitive coupling between two areas. Insulation of all crossing conductors and grounded connections are also needed in this case to suppress harmful induced eddy currents [12].

For the study, variants (b) and (c) were chosen. To investigate variant (b), respectively the parallel wire loops, a flat ribbon cable, common in computer applications, was chosen. Not only because of its already existing insulation between the single wires and the surrounding, but also because of its ease of the grounding possibility and very straight and accurate parallel wire distribution inside. For the overhang-shielding variant (c), a very fine mesh, embedded in between two insulation foils, is used. The mesh width of the shielding is far below the critical wavelength. The analytical formula of the critical wavelength in (4), in which c describes the propagation speed of waves, can estimate the minimum mesh width [14].

$$\lambda_{\text{crit}} = \frac{c}{f_{\text{crit}}} \tag{4}$$

The shielding effect in the far field, for which the mesh width is important, must be considered. A very small mesh width prevents electromagnetic waves from passing through the shielding. Hence, only if the hole size is of the same order as the wavelength, these waves can propagate through [14]. E.g. for electromagnetic waves of frequencies up to $500\,\text{MHz}$, the critical wavelength in free space is $599.58\,\text{mm}$.

IV. Validation Setup

The effectiveness of the developed shieldings are validated by impedance measurements. A Keysight E4990A Impedance Analyzer, which can measure the capacitance in a range between $20\,\text{Hz}$ and $50\,\text{MHz}$, was employed. Moreover, a test support for the slot-shieldings, which is shown in Fig. 4(a), was developed.

The important parts are a socket for the motorettes and a alignable conductive cylinder, which is representative for the rotor in an electric machine For the validation of the overhang shieldings, another rotor substitute was built. As presented in Fig. 4(b), it is also a conductive cylinder, which is inserted into the correspondent stator.

V. FEA Results of the Shielding Designs

In the following section, the above-presented shielding types, the slot-shieldings and the overhang-shielding are analyzed with help of Finite Element (FE)-simulations. In addition to the electrostatic field simulation to gather the capacitance values, a magnetic Finite Element Analysis (FEA) was adapted to compute the additional losses due to eddy currents in the shieldings.

A. Slot-shielding

The electrostatic field simulations for the reference design were realized in 3D and 2D. Since its deviation is below $1\,\%$, the FE-simulations for the slot shielding variants only need to be calculated in 2D. In Fig. 5 the electric field calculated by the 2D electrostatic FE-simulation is shown.

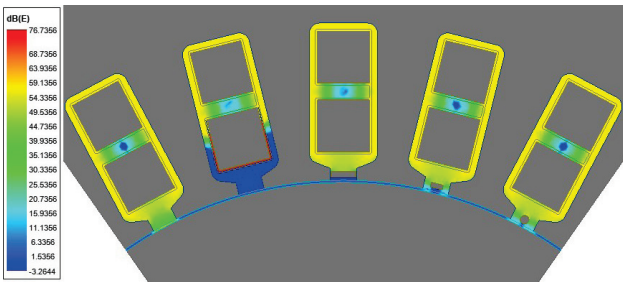

Fig. 5: Electric field FE-simulation result of the motorette with embedded slot-shieldings

The reference slot, leftmost, shows clearly the unimpeded electric field which forms a capacitance between the winding and the rotor C_{WR}. The second and third slot with the copper foil, respectively copper strip inside shield the electric field almost completely, while the shieldings in slot four and five allow the propagation of a remaining field. Clearly can be seen, that the flat copper shielding in slot four is more effective than the round copper wire in slot five. Reasoning can be made by the already shown analytical estimation in (3), in which the magnitude of $(b_{\mathrm{Slot}} - b_{\mathrm{Sh}})$ has a strong influence on it. The magnitude of the resulting deviation of the capacitance between the winding and the rotor of one slot from the reference slot ΔC_{WR} is presented in Table II.

TABLE II: Deviation of the capacitance ΔC_{WR} determined by the FE-simulation of the motorette with embedded slot-shieldings

Description	***Slot 2***	***Slot 3***	***Slot 4***	***Slot 5***
Type	Foil	Strip	Flat wire	Round wire
ΔC_{WR} in fF	-584.30	-584.30	-576.99	-538.29
ΔC_{WR} in %	100	100	98.75	92.13

Comparing the effectiveness of the shielding in the slots three and four, the difference is only $1.8\,\%$ despite the fact that the shielding in four is $2.5\,\mathrm{mm}$ narrower. This result shows that, unlike the analytical estimation, the width of the slot-shieldings contribute non-linearly to the shieldings' effectiveness.

The additional variant with the embedded conductive glow protection material has the same geometry as the copper foil in slot two, hence it is evident that an FE simulation shows that this variant shields the electric field just as well.

The second FEA, a magnetic eddy current simulation, determined the additional losses caused by slot shielding in the motor. In general, the losses of the machine can be divided into copper-, iron-, eddy current-, hysteresis- and additional losses. Since only the additional eddy current and copper losses are of interest in this study, the other loss types are neglected in the following. In summary, the FEA results in Table III indicate that the additional losses in an electrical machine with slot-shieldings are below $2\,\%$ in comparison to the corresponding original motor.

TABLE III: Additional losses in the motor determined by FEA of the original motor with and without embedded slot-shieldings

Description	***Slot 2***	***Slot 3***	***Slot 4***	***Slot 5***
Type	Foil	Strip	Flat wire	Round wire
$\Delta P_{\mathrm{copper}}$ in W	59.6	11.5	2.98	3.56
ΔP_{eddy} in mW	300	5.2	0.04	0.3
ΔP_{sum} in W	59.6	12.2	3.02	3.59
ΔP_{sum} in %	1.34	0.248	0.059	0.089

The additional variant with the embedded conductive glow protection foil is far below the losses of its equivalent shielding geometry made of copper. This is due to the fact that the conductivity of copper is much higher compared to glow protection material.

B. Overhang-shielding

To assess the capability of the overhang shielding, 3D electric field FE-simulations were used to calculate the capacitance between the bent conductors and the rotor.
The results in Table IV show that both variants are very effective in reducing the capacitance between the winding and the rotor in the overhang part.

TABLE IV: Deviation of the capacitance ΔC_{WR} determined by the FE-simulation of the motorette with embedded slot-shieldings

Description	***Flat ribbon cable***	***Fine meshed faraday's cage***
ΔC_{WR} in pF	-109.82	-114.01
ΔC_{WR} in %	82.7	84.8

A 3D eddy current simulation for the overhang part has an enormous computational effort. Since this part of the winding is surrounded by air, the flux density in this area is very small, and thus, the induced eddy currents are very small, hence negligible. Consequently, an analytical assessment of those due to [10] is appropriate and the computation of them is superfluous.

VI. Validation

In the following, the validation of the different shieldings' effectiveness is presented. The measurement setup for the validation is already presented in Section IV. For both shielding types, slot- and overhang-shielding, the impedance analyzer was used to measure the capacitance C_{WR} between the winding and the rotor substitute in a frequency range between $10\,\mathrm{kHz}$ and $1\,\mathrm{MHz}$. In post-processing, the mean value of the capacitance measurement results was calculated, so that a single value of C_{WR} can be compared in the following.

A. Slot-shielding

In Fig. 6a the built motorette with the four different slot-shielding variants, which were investigated simulatively in Section V-A, is presented.

The results of the measurements, but also those of the simulation are given in the Fig. 7. The bar chart shows, that both, simulation and measurement indicate a large reduction of the winding-rotor-capacitance C_{WR}. Further, it indicates

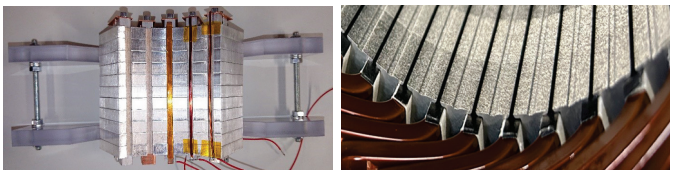

(a) Motorette with four different slot-shielding variants

(b) Slot-shielding with conductive glow protection foils

Fig. 6: Slot shielding variants

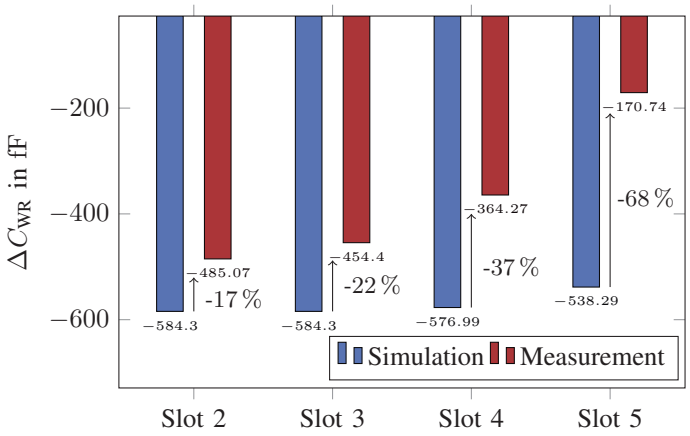

Fig. 7: Simulation and measurement result of the different slot-shielding variants

that the reduction, determined by FEA for the round wire shielding is approx. 68 % higher than the measured reduction. The error of the other shieldings is below 37 %. On the one hand side, the large difference between the measurement and the simulation can be explained by the influence of the measurement setup. The impedance analyzer's clamps itself may create an additional parasitic capacitance or the thin wires used for grounding may also affect the measurements. On the other hand side, the error is due to the 2D simulations. Those can not consider the winding overhang of the motorette and its connection to the impedance analyzer.

Nevertheless, the simulations and measurements match qualitatively. In both cases, the effectiveness of all slot-shielding variants is validated. Further, both results show the highest effectiveness for the copper foil. Unsurprisingly, the round wire is the least effective. Reasoning can be derived from Fig. 5. The magnitude of the remaining electric field between the winding and the rotor is the highest, compared to all other slots.

In Fig. 6b the motorette of the slot-shielding variant with the embedded conductive glow protection foils are presented. It depicts that there is a direct contact between the slot shielding and the stator lamination stack, which is equivalent to a slot wedge, often used in large synchronous generators [15]. Since the foil is in contact with the stator along its entire stack length, there's no need for an additional grounding of the shielding.

The measurements show a possible reduction in the winding-rotor-capacitance C_{WR} of approx. 416.08 fF per slot respectively 71.21 %, while the 2D simulation calculates a complete mitigation of the electric field. The error can be explained analogous to the measurement errors, already explained above in context of the other slot-shielding variants.

B. Overhang-shielding

In Fig. 8 the two built stators of the corresponded motor with the two simulatively investigated overhang-shielding variants in Section V-B are presented.

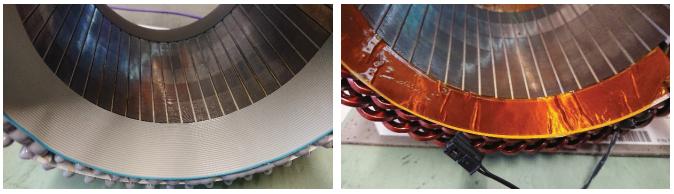

(a) Overhang shielding with a flat ribbon cable (b) Overhang shielding with a fine-meshed Faraday's cage

Fig. 8: Overhang-shielding variants

The simulated and measured effectiveness results are compared in Fig. 9. The bar chart confirms for both variants and both calculation methods a large reduction of the parasitic capacitance between the winding and the rotor.

It depicts that the fine mesh Faraday's cage has due to both determination types the higher effectiveness. The errors between the simulation and the measurement results are below 2 %. In comparison to the slot-shielding results, the simulations are more accurate, since they are built in 3D.

The difference between both shielding variants is approx. 2 %. It can be concluded that both variants are suitable approaches to mitigate the electric field between the winding and the rotor in the overhang part of a motor.

C. Discussion

The study shows for both, slot- and overhang-shieldings a great effect on the electric field between the winding and the rotor in an electric machine. For the final series design, it is important that the shielding complies with all standards, especially the DIN EN 60204-1 and IEC 60034-18-41 norms [13], [16]. The copper wire slot shielding variant may conflict with safety requirements, so the conductive glow protection foil is considered as the more suitable solution. In further work, insulated copper variants could be investigated since they have offered a promising potential to reduce the winding-rotor-capacitance C_{WR} effectively and therefore also to reduce the BVR, hence the harmful capacitive bearing currents.

The investigated two overhang shielding variants are seen also as very effective and can strongly contribute to the reduction of the known parasitic effects. However, when specifically applied to an electrical machine, the final design of the entire overhang must be taken into account. The windings'

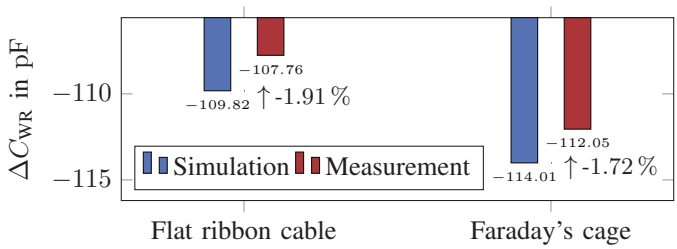

Fig. 9: Simulation and measurement results of the different overhang-shielding variants

distance from the rotor or its end plates in the overhang may be too large, resulting in an insignificant reduction of the electric field, hence becoming superfluous. The safety requirements due to the above mentioned DIN EN 60204-1 and IEC 60034-18-41 standards [13], [16] must be fulfilled also in the overhang part. Further, the study found that both overhang-shielding options lead to a significant reduction, and that the induced eddy currents are very small.

Further work must include the investigation of the temperature in the shielding variants. The losses in the shieldings calculated by FEA are quite small. According to a first assessment by (5), in which P_{loss} is the total loss, m_{shield} denotes the mass, and c_{shield} describes the specific thermal capacity of the shieldings, a temperature rise below $0.09\,\mathrm{K\,s^{-1}}$ is calculated [10].

$$\frac{\mathrm{d}T}{\mathrm{d}t} = \frac{P_{\text{loss}}}{m_{\text{shield}} \cdot c_{\text{shield}}} \tag{5}$$

The temperature rise seems to be in an acceptable range, so that the electric machine will not be destroyed. Lastly, the slot-shieldings' effect on the machines' efficiency and cost must be investigated. In the very competitive market, especially in the traction segment, power density and cost become crucial.

D. Conclusion

In summary, this paper investigates different measure variants to shield the electric field between the winding and the rotor. Both parts, stator and overhang are taken into account. The methods to investigate the shieldings are FEA and equivalent motorettes were built so that the FEA results are validated.

Some designs show a complete mitigation so that the shielding can avoid shaft voltages and hence harmful capacitive bearing currents. The investigation not only focuses on the magnitude of the capacitance reduction between the winding and the rotor, it addresses also the additional losses caused by the shieldings.

Finally, the study concludes that a thin conductive and grounded film near the slot opening, combined with a grounded fine meshed Faraday's cage in the overhang, effectively shields an electric motor from harmful parasitic effects. Future work involves integrating this shielding into a complete motor prototype to validate the built motorettes.

References

[1] B. Shi, A. I. Ramones, Y. Liu, H. Wang, Y. Li, S. Pischinger, and J. Andert, "A review of silicon carbide mosfets in electrified vehicles: Application, challenges, and future development," vol. 16, no. 12, pp. 2103–2120, 2023.

[2] E. C. Wittek, *Charakterisierung des Schmierungszustandes im Rillenkugellager mit dem kapazitiven Messverfahren*. Hannover : Gottfried Wilhelm Leibniz Universität Hannover, 2017.

[3] A. Muetze and A. Binder, "Don't lose your bearings," vol. 12, no. 4, pp. 22–31, 2006.

[4] Dyson, A., Naylor, H. and A. R. Wilson, "The measurement of oil-film thickness in elastohydrodynamic contacts," in *Proceedings of the Institution of Mechanical Engineers, Conference Proceedings*, vol. 180, 1965, pp. 119–134.

[5] D. Macdonald and W. Gray, "A practical guide to understanding bearing damage related to pwm drives," in *Conference Record of 1998 Annual Pulp and Paper Industry Technical Conference (Cat. No.98CH36219)*. IEEE, 1998, pp. 159–165.

[6] K. Vostrov, J. Pyrhonen, P. Lindh, M. Niemela, and J. Ahola, "Mitigation of inverter-induced noncirculating bearing currents by introducing grounded electrodes into stator slot openings," vol. 68, no. 12, pp. 11 752–11 760, 2021.

[7] H. W. Oh and A. Willwerth, "Shaft grounding-a solution to motor bearing currents," vol. 114, pp. 246–251, 2008.

[8] M. T. Alves Êvo and H. Paula, "Electrostatic shielding for bearings discharge currents attenuation: analysis of its effectiveness, losses and impact on the motor performance – a study for design guidelines," vol. 14, no. 6, pp. 1050–1059, 2020.

[9] VDE-Verlag, *VDE 0530-25:2018-12 (IEC/TS 60034-25:2014) Drehende elektrische Maschinen*.

[10] B. Heidler, K. Brune, and M. Doppelbauer, "Design aspects of an electrostatic shield in an electric machine for hybrid electric vehicles," in *8th IET International Conference on Power Electronics, Machines and Drives (PEMD 2016)*, 2016.

[11] B. Heidler, *EMV-gerechte Gestaltung einer elektrischen Maschine für Hybrid- und Elektrofahrzeuge*. Cuvillier Verlag, 2017.

[12] K. Vostrov, J. Pyrhonen, and J. Ahola, "Shielding the end windings to reduce bearing currents," pp. 1431–1437, 2020.

[13] VDE-Verlag, *DIN EN 60204-1 VDE 0113-1:2019-06 Sicherheit von Maschinen – Elektrische Ausrüstung von Maschinen*.

[14] H. A. Wolfsperger, *Elektromagnetische Schirmung*, ser. VDI-Buch. Springer, 2008.

[15] Y. Xiao, L. Zhou, J. Wang, and J. Liu, "Design and performance analysis of magnetic slot wedge application in double fed asynchronous motor generator by finite element method," 2018.

[16] VDE-Verlag, *DIN EN 60034-18-41 VDE 0530-18-41:2021-05 Drehende elektrische Maschinen*.

VII. Biographies

Silvan Scheuermann was born in Pforzheim, Germany. He received his M.Sc. degree in automotive engineering from the Technical University Munich (TUM) in 2020. He is currently working as a research associate with the Institute of Electrical Engineering (ETI) at the Karlsruhe Institute of Technology (KIT). His research interests include investigation, modeling, and beneficial design of electrical machines as well as the analytical determination of parasitic effects in drives and measures against them.

Dr.-Ing. Matthias Brodatzki was born in Bytom, Poland in 1988. He received his M.Sc. degree in electrical engineering from the Karlsruhe Institute of Technology (KIT) in 2014. He achieved his doctorate degree at the Institute of Electrical Engineering (ETI) and is now research group leader with this institute in the field of electrical machines and drives.

Prof. Dr.-Ing. Martin Doppelbauer was born in Altenhundem in Germany. He graduated at the Technical University in Dortmund, where he received his doctorate degree in 1995. From 1995 to 2010 Prof. Doppelbauer worked at Danfoss Bauer and at SEW Eurodrive in the field of industrial electric motor development. Since 2011 he holds the chair of hybrid and electric vehicles at the Karlsruhe Institute of Technology (KIT). His research interest is the electrical drive train of vehicles with a particular focus on electric machines with high power density. Prof. Doppelbauer is actively involved in standardization as the chairman of the TC2 (Rotating Machinery) of the International Electrotechnical Commission (IEC).